

Inelastic Scattering from $^{20}\text{Ne}^*$

K. Amos,^A L. Berge,^A C. Steward^A and R. de Swiniarski^B

^A School of Physics, University of Melbourne, Parkville, Vic. 3052, Australia.

^B Institut des Sciences Nucléaires, Université de Grenoble,
38026 Grenoble Cedex, France.

Abstract

Inelastic scattering of 800 MeV protons exciting states of the ground state rotation band of ^{20}Ne is studied using large basis space, microscopic model (Hartree–Fock) wavefunctions and free two-nucleon t -matrices, one of which is based upon the Paris interaction. Results are compared with coupled channels analyses of the data made using Dirac as well as Schrödinger phenomenology. Thereby it is suggested that coupled channels effects in the reaction mechanism are essential in analysis of such higher energy reaction data.

1. Introduction

The wavefunctions of nuclear states are usually assessed by comparing their associated eigenvalues and predictions of electromagnetic transition probabilities with experimental data. Frequently fits to the latter require the use of effective charges for the nucleons within the nucleus. Good reproduction of such data with small effective charges, makes credible the model predictions of the charge distribution and (low) multipole transition moments, the crucial many-nucleon factors in which are one body transition density matrix elements (OBDME) (Millener *et al.* 1989).

Reliable OBDME values can be obtained without any conceptual difficulties whenever an adequate many-nucleon basis is used in an appropriate microscopic structure model. For light nuclei, e.g. the p-shell and s–d shell nuclei, the conventional shell model is quite reasonable (Amos *et al.* 1989*a*, 1989*b*, and references cited therein), although basis truncation effects can be severe for description of any states with appreciable collectivity. For some cases (the ground state rotation bands of $4N$ nuclei for example), the collective states can be well represented as projections out of the single basis determinant from Hartree–Fock theory. In light nuclei with large state quadrupole moments that technique has been very successful. In particular, the ground state rotation band of ^{20}Ne , of specific interest herein, is well described thereby (Ford *et al.* 1971; Nesci and Amos 1977).

Complementary, and perhaps more stringent, tests of OBDMEs and the associated (radial) transition form factors are provided by their use in analyses of direct reaction hadron inelastic scattering, since such reactions are mediated

* Dedicated to Professor Ian McCarthy on the occasion of his sixtieth birthday.

by the strong short range nuclear force. Thereby, they are sensitive to both proton and neutron distributions. Further, as all multipole transition moments are comparable, data should be, and frequently are, available from excitations involving large angular momentum transfer values. To effect large angular momentum transfer values often means that the final states from reactions have special, simple structures such as the so-called 'stretched' states. But the short range nature of the two-nucleon t -matrix is also a reason why analyses of inelastic scattering data using collective model representations yield deformation parameters that agree well, usually, with those extracted from measured (ground state) γ -decay rates. Here we consider inelastic nucleon scattering to such collective states, namely to the 2_1^+ and 4_1^+ states of the ground state rotation band of ^{20}Ne .

The distorted wave approximation (DWA) is most appropriate to use in the direct reaction theory of intermediate energy inelastic scattering of nucleons from nuclei. As yet, however, it is a computational necessity to choose to analyse data using either a collective model or a microscopic model prescription of the reaction process. In the former, channel coupling and deformed field effects can be considered and with both Schrödinger and Dirac equation solutions for the 'distorted waves' (Raynal 1987, 1988). But coupled channels calculations do not as yet account specifically for totally antisymmetrised state vectors, associated with which are exchange scattering amplitudes that are known to be important (Amos *et al.* 1988). For the transitions within ^{20}Ne and induced by 800 MeV protons, recent analyses of the data (Blanpied *et al.* 1988; Pham and de Swiniarski 1990) were made using such a coupled channels method, the most recent using Dirac phenomenology. Excellent fits to the data were obtained. Here we consider the same data, but investigate the reactions using the microscopic model viewpoint.

The microscopic model DWA approach to the analysis of inelastic scattering requires specification of the two-nucleon t -matrices that promote the transition, as well as of the OBDME values from microscopic models of nuclear structure. At low to intermediate projectile energies (e.g. <300 MeV), those t -matrices differ markedly from the free N-N t -matrices due to the presence of the nuclear medium (von Geramb 1983). Both Pauli blocking and an average field in which the nucleons propagate cause the N-N t -matrices within the medium to be energy and density dependent at the very least. There is also some variability caused by the choice of N-N interaction with which to start calculations of the t -matrices. Eventually, one hopes to start with interactions ascertained by inversion of two-nucleon scattering data (von Geramb and Amos 1990) and to solve the (infinite) nuclear matter t -matrix equations using full Pauli blocking and a mass operator which is as complete as possible. At present, however, model energy and density dependent t -matrices must suffice. But at higher energies, for example 800 MeV, such medium corrections should be of considerably less significance, whence the free N-N t -matrices can be used in scattering analyses. There is a problem then of whether or not the starting N-N interactions are reliable. Here we consider t -matrices deduced from the Paris interaction (Lacombe *et al.* 1980) and we compare results obtained using them in DWA calculations with those obtained using model t -matrices as specified by Love and Franey (1981, 1985). In all DWA calculations the Schrödinger equation is solved to give the distorted waves, albeit that relativistic kinematics are

used. As noted earlier, solutions of the Dirac equation are not an option as yet in computer codes. However, full account is taken of antisymmetrisation with explicit exchange scattering amplitudes being evaluated. Such studies, we note, have been standard from the early 1960s (Amos and McCarthy 1963).

Details of the elements used in our calculations are given in the next section, while the results and a discussion are presented in Section 3.

2. Details of Calculations

In the microscopic model DWA for direct reaction inelastic scattering of protons from nuclei, the scattering amplitudes are given by

$$T_{if} = \sum_{\alpha j_1 j_2 l} S_{j_1 j_2}^{(\alpha)} C_{j_1 j_2 l} \langle \chi_f^{(-)}(1) \phi_{j_2}(2) | t(12) | \{ \chi_i^{(+)}(1) \phi_{j_1}(2) - \chi_i^{(+)}(2) \phi_{j_1}(1) \} \rangle, \quad (1)$$

where the OBDMs are defined* by

$$S_{j_1 j_2}^{(\alpha)} = \langle \Psi_{J_f} | [a_{j_2}^\dagger \times a_{j_1}]_{(\alpha)}^l | \Psi_{J_i} \rangle. \quad (2)$$

The algebraic coefficients are collectively represented by $C_{j_1 j_2 l}$, the χ^\pm are the projectile-nucleus (optical) model wavefunctions and $t(12)$ is the two-nucleon t -matrix that promotes the transition. With $\phi_j(q)$ representing single-nucleon wavefunctions and with the OBDMs defined above, the $B(EI)$ values for electromagnetic transition rates and the form factors from electron scattering are given by

$$B(EI) = \{(2I+1)(2J_f+1)\}^{-1} \left| \left(\sum_{j_1 j_2 \alpha} e_\alpha S_{j_1 j_2}^{(\alpha)} \langle \phi_{j_2} | r^l Y_l | \phi_{j_1} \rangle \right) \right|^2, \quad (3)$$

$$|F_l^{(x)}(q)|^2 = \{4\pi/Z^2(2I+1)(2J_i+1)\} f_{\text{recoil}} \times \left| \left(\sum_{\alpha j_1 j_2 L} S_{j_1 j_2}^{(\alpha)} \langle \phi_{j_2}^{(\alpha)} | X_{Ll}^{(x)}(q) | \phi_{j_1}^{(\alpha)} \rangle \right) \right|^2. \quad (4)$$

We use x to signify longitudinal, transverse electric or transverse magnetic multipole operators for $X_{Ll}^{(x)}(q)$ as is relevant. In these operators one finds e_α (the effective charge of nucleon of type α **) and $g_l^{(\alpha)}$, $g_s^{(\alpha)}$ (the effective g factors). Details of these operators are not essential for the discussion here, but they can be deduced easily using the specifications given by Cheon (1983). Our interest lies with the excitation of the 2_1^+ and 4_1^+ states of ^{20}Ne , whence with J_i zero, l is equal to J_f . Also, there are then no magnetic form factors to be considered.

The low excitation spectrum of ^{20}Ne and transition rates between the states therein have been calculated using the conventional s - d shell model, as well as projected Hartree-Fock (PHF) models of varying dimension (Ford *et al.*

* These were defined as spectroscopic amplitudes in earlier work (Amos and Bauhoff 1984; Nesci and Amos 1977).

** A polarisation charge is defined by $\delta e_i = e_\alpha - e_i$ where e_i is the bare charge.

1971; Nesci and Amos 1977). The OBDMEs have been published in table form (Nesci and Amos 1977) and are not repeated here. The same labels are used however to identify the results obtained with different sets of OBDME values. Specifically SM, s-d PHF and full PHF identify results obtained with shell model, with s-d shell basis (or s-d shell components of) PHF calculations and with 0s-0g single particle space PHF values respectively. Some of those (spectroscopic) amplitudes have been used (Amos and Bauhoff 1984; Amos and Steward 1990) to consider electron and proton scattering; the latter at low energies.

The γ -decay rates, as with the other transition form factors and scattering amplitudes, involve the single-nucleon wavefunctions $\phi_j(r)$. We have used harmonic oscillator wavefunctions for these in our calculations ($\hbar\omega = 11.2$ MeV). While Woods-Saxon functions would be more realistic (Millener *et al.* 1989), the 0s-0g basis PHF studies were based upon harmonic oscillator functions and it is difficult to know what Woods-Saxon parameters to use for such a large space of single-nucleon states. With the oscillator functions, the $B(E2)$ values obtained using the SM, s-d PHF and full PHF structure models required polarisation charges of $0.33e$, $0.28e$ and $0.11e$ respectively. The full PHF $B(E4)$ value required a value of just $0.07e$. These values reflect that the ground state band is well approximated by a prolate axially symmetric structure. The electron scattering form factors, to be discussed in the next section, confirm that effect and so the same structures were used in analyses of the proton inelastic scattering data.

Table 1. DWA and coupled channels optical model parameters

Parameter	DWA	Coupled channels	Parameter	DWA	Coupled channels
V	-1.0	-5.0	V_{so}	2.0	0.0
r	0.95	1.06	r_{so}	0.95	0.0
a	0.69	0.46	a_{so}	0.66	0.0
W	59.3	48.0	W_{so}	0.78	0.0
r_w	0.95	1.06	r_c	1.05	1.05
a_w	0.69	0.46			

Besides the structure data, DWA scattering amplitudes involve scattering wavefunctions and two-nucleon t -matrices. Of necessity, the former are generated as solutions of the Schrödinger equation with conventional optical model potentials, albeit that at 800 MeV relativistic kinematics are used. We made a search to best fit the elastic data and obtained the parameter values listed in Table 1. However, recent studies (de Swiniarski *et al.* 1988; Pham and de Swiniarski 1990) suggest that Dirac phenomenology is more appropriate. Those studies involved channel coupling and collective representations of structure, and so no explicit treatments of exchange amplitudes were made. The effects of antisymmetrisation are not negligible at 800 MeV (Amos *et al.* 1988). Also, with our large basis structure models of spectroscopy, channel coupling was not necessary to predict electron scattering form factors (Amos and Steward 1990). For completeness, the values of the (Schrödinger) coupled channels potential parameters are also listed in Table 1.

At 800 MeV incident energy, medium corrections to the N-N t -matrices should be far less significant than at 200 MeV or below. Hence, we choose

Table 2. 800 MeV Love-Franey interaction (LF81)

(fm)	$S=0, T=1$	$S=1, T=0$	$S=0, T=0$	$S=1, T=1$
	Central real			
0.15	-1.596×10^4	-2.045×10^4	2.702×10^5	-1.096×10^5
0.25	9.130×10^3	8.359×10^3	-6.042×10^4	2.712×10^4
0.40	-1.382×10^3	-6.089×10^2	4.753×10^3	-2.392×10^3
1.40	-1.050×10^1	1.050×10^1	3.150×10^1	3.500
	Spin-orbit real		Tensor real	
0.11			-2.248×10^6	-7.461×10^5
0.15	3.854×10^4	6.787×10^3	5.294×10^5	1.973×10^5
0.25	-5.555×10^3	-2.162×10^3	-1.542×10^4	-5.016×10^5
0.40	1.400×10^2	-1.435×10^2		
0.70			-4.687×10^1	1.732×10^1
	Central imag.			
0.15	1.544×10^4	-8.160×10^3	-9.421×10^4	5.921×10^3
0.25	-4.747×10^3	5.397×10^3	1.800×10^4	-1.334
0.40	-2.886×10^2	-1.202×10^3	1.560×10^3	-9.480×10^2
	Spin-orbit imag.		Tensor imag.	
0.11			-3.575×10^5	-9.602×10^5
0.15	1.285×10^4	-3.596×10^3	1.290×10^5	2.336×10^5
0.25	-9.188×10^1	2.081×10^3	-2.625×10^3	-7.082×10^3
0.40	9.467×10^1	-4.609×10^1		
0.70			1.252	2.569

Table 3. 800 MeV Love-Franey interaction (LF85)

(fm)	$S=0, T=1$	$S=1, T=0$	$S=0, T=0$	$S=1, T=1$
	Central real			
0.15	-4.270×10^4	-1.162×10^4	-1.748×10^5	-1.092×10^5
0.25	2.108×10^4	4.962×10^3	-4.026×10^4	2.754×10^4
0.40	-2.777×10^3	-2.469×10^2	3.512×10^3	-2.428×10^3
1.40	-1.050×10^1	1.050×10^1	3.150×10^1	3.500
	Spin-orbit real		Tensor real	
0.11			-1.744×10^6	-5.846×10^5
0.15	6.215×10^3	2.203×10^4	4.195×10^5	1.401×10^5
0.25	-1.565×10^3	-5.310×10^3	-1.322×10^4	-3.320×10^3
0.40	1.266×10^2	5.534×10^1		
1.40			-4.967×10^1	1.786×10^1
	Central imag.			
0.15	2.855×10^3	-1.616×10^4	-6.185×10^4	9.231×10^3
0.25	1.024×10^3	8.881×10^3	1.278×10^4	-1.274×10^3
0.40	-9.962×10^2	-1.666×10^3	-1.261×10^3	-7.835×10^2
	Spin-orbit imag.		Tensor imag.	
0.11			-4.312×10^5	-8.213×10^5
0.15	-1.720×10^4	3.199×10^3	1.444×10^5	1.959×10^5
0.25	2.564×10^3	1.048×10^3	1.356×10^3	-6.587×10^3
0.40	2.711×10^1	-4.513×10^1		
1.40			1.082	2.815

to use 'free' N-N t -matrices. Specifically we have used those given by Love and Franey (1981, 1985), and a set that we have determined from the exact (on- and off-shell) values of N-N t -matrices based upon the Paris interaction.*

* This determination was made with the collaboration of Professor H. V. von Geramb and his group at the University of Hamburg. Note that 387 MeV t -matrices were used as 800 MeV data were not available.

Table 4. 387 MeV free Hamburg interaction (Ham90)

(fm)	$S=0, T=1$	$S=1, T=0$	$S=0, T=0$	$S=1, T=1$
			Central real	
0.25	4.022×10^3	4.028×10^3	1.669×10^4	7.930×10^3
0.35	-4.209×10^3	-3.110×10^3	-1.901×10^4	-5.882×10^3
0.52	1.474×10^3	4.478×10^2	6.076×10^3	1.302×10^3
1.41	-6.912	-2.701×10^1	-2.890×10^2	-3.429×10^1
			Tensor real	
0.25	-2.460×10^4	1.565×10^3	5.022×10^3	1.474×10^3
0.35	1.357×10^4	-1.439×10^3	-2.716×10^3	-8.009×10^2
0.52	-2.252×10^3	1.682×10^2		
0.55			2.990×10^2	2.941×10^2
0.70			-2.017×10^1	-8.533×10^1
			Central imag.	
0.25	1.188×10^3	-3.406×10^3	-2.928×10^3	-1.430×10^2
0.35	-8.221×10^2	3.771×10^3	4.067×10^3	1.107×10^2
0.52	-5.893×10^1	-1.131×10^3	-1.543×10^3	-1.687×10^2
1.41	1.073×10^1	3.176×10^1	4.270×10^1	1.138×10^1
			Tensor imag.	
0.25	2.105×10^3	2.022×10^3	-2.021×10^2	-1.187×10^3
0.35	-9.347×10^2	-1.105×10^3	5.727×10^2	4.016×10^2
0.52	1.912×10^2	1.533×10^2		
0.55			-2.563×10^2	-4.773×10^1
0.70			6.932×10^1	6.822

All three t -matrices are cast in the form of complex, linear combinations of Yukawa functions associated with central, two body spin-orbit and tensor operators. The parameter values of these forces are listed in Tables 2, 3 and 4. All involve compensating attractive and repulsive terms of different ranges and are identified by LF81, LF85 and Ham90 hereafter. The LF81 and LF85 interactions are qualitatively similar; both are tailored to fits to some nuclear scattering data at intermediate energies but within a dynamically nonrelativistic framework. The LF85 set was calculated to update the LF81 effective interaction and is based on the SP84 N-N amplitudes of Arndt *et al.* (1983); these were deduced from analyses of considerably more N-N data at intermediate energies than were the set of amplitudes upon which the LF81 interaction is based. The effective t -matrices were then obtained by modulations that gave fits to select (pp') data. At 500 MeV, it was shown that in certain transitions [$0^+ \rightarrow 1^+$ ($T=0$) in ^{12}C] there are significant differences in predictions of spin observables from DWA calculations made using the two effective t -matrices. In many cases, however, and for reactions initiated by protons with energies in the range 120 to 800 MeV, both the LF81 and LF85 sets of effective t -matrices give quantitatively similar results (Love and Franey 1981, 1985). The Ham90 effective t -matrix was obtained by mapping the chosen structural form to best fit the fully off-shell t -matrices calculated from the Paris interaction (Lacombe *et al.* 1980). The mapping was achieved using a singular value decomposition of interaction matrices by which (a finite set of) ranges and strengths could be varied to give a best fit. No variation in those parameters of the potential to account for nuclear medium or reaction process effects, for example, has been made. We only have t -matrices and the functional forms mapped to them for energies up to 387 MeV. Thus we

have used the largest energy cases and assume that they are appropriate for all higher energies. To the extent that the LF81 and LF85 model t -matrices are appropriate, the Ham90 results in comparison should then indicate the effects of energy variation in the regime for which the t -matrices should not be severely affected by medium corrections.

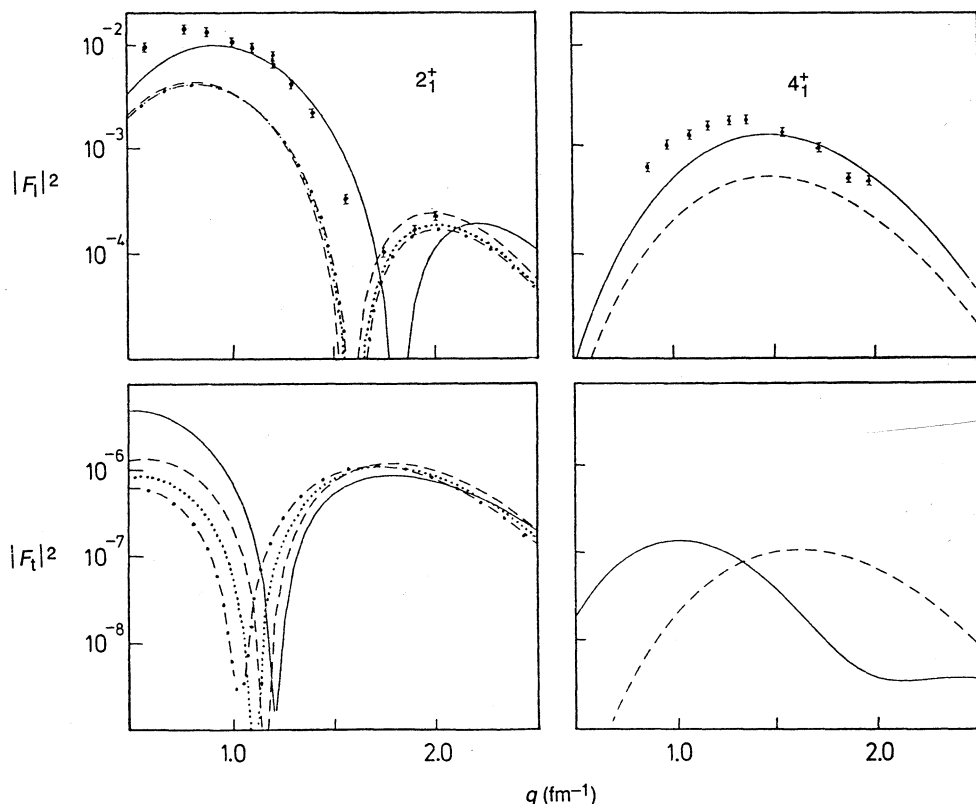


Fig. 1. Electron scattering form factors from the excitation of the 2_1^+ and 4_1^+ states in ^{20}Ne . The longitudinal and transverse electric form factors are shown in the top and bottom sections for the 2_1^+ and 4_1^+ excitations. The curves are identified in Section 3.

3. Results

The electron scattering form factors from excitation of the 2_1^+ and 4_1^+ states of ^{20}Ne are shown in Fig. 1. The longitudinal form factors, for which data exist (Horikawa *et al.* 1971), are presented in the top section, while the transverse electric form factors calculated using various models of nuclear structure are displayed in the bottom section. The results of calculations made using the large basis PHF model of nuclear structure are shown by the continuous (full spectroscopy) and dashed (s - d shell components) curves. The dot-dash and dotted curves represent the results obtained previously using the shell model and deformed shell model OBDMEs for the 2_1^+ excitation (Amos *et al.* 1980). In all calculations, harmonic oscillator functions ($\hbar\omega = 11.2$ MeV) were used.

Comparison of the results with both the 2_1^+ and 4_1^+ longitudinal form factor data shows clearly that only the large basis space calculations give reasonable

magnitudes. All of the *s*-*d* space calculations need substantial core polarisation corrections. Furthermore, the *s*-*d* space results all are similar and different to the large basis space result in the momentum dependence of the 2_1^+ form factor. Again the large basis space calculation gives the best result. A slightly smaller value for the oscillator energy could improve agreement with the data but, in view of the results for the 800 MeV (*pp'*) data analyses to be discussed, such a variation is of small consequence. Essentially the large basis PHF model of structure gives the electromagnetic attributes of the ground state rotation band in ^{20}Ne . A more sensitive test of the models of structure would be a comparison of the transverse electric form factors with measured data. Our calculations show that, for the 4_1^+ excitation particularly, the large basis space structure yields form factors distinctively different from any of the results of calculations using *s*-*d* based spectroscopy. These results also correct an error made in our earlier calculations (Amos and Steward 1990).

Thus, it was with expectation of reasonable fits to data that microscopic models of structure were used in DWA calculations using fully antisymmetrised wavefunctions and 'realistic' effective two-nucleon *t*-matrices to evaluate cross sections and analysing powers for 800 MeV (\vec{p}, p') scattering. The three different *t*-matrices as specified earlier were used to obtain the results shown in Figs 2 and 3 for the 2_1^+ and 4_1^+ transitions respectively. The results obtained using the LF81, LF85 and Ham90 interactions are displayed in the top, middle and bottom panels respectively. In view of the reasonable fits to data obtained using the full PHF model of structure for the electron scattering form factors, as well as in analyses of low energy (24.5 MeV) inelastic scattering data (Amos and Bauhoff 1984), our calculations for 800 MeV scattering give surprisingly poor results when compared with the data.

The results for the microscopic model calculation for the 2_1^+ excitation are displayed in Fig. 2. The curves represent the same calculations as in Fig. 1. The general variation in the cross sections with different structure model input reflect the magnitude variations of the longitudinal form factors (Fig. 1), while the absolute magnitudes scale as the net strengths of the three *t*-matrices. The calculated differential cross sections are all similar in shape and, although that shape is characteristic of the data, it is not a fit to the observed variation. Thus, there appears to be a problem with the reaction mechanism assumed in these DWA calculations. In part we can attribute this to inadequacies in the selected two-nucleon *t*-matrices; the failure to give even a shape similar to the analysing power data illustrates this problem with the LF81 and LF85 forces.

The 4_1^+ excitation data are compared in Fig. 3 with the results obtained using the full PHF and *s*-*d* components of the PHF model of nuclear structure. There is a consistency between these results and the associated calculated electron scattering form factors as the same core polarisation scale factors relate *s*-*d* to full basis cross sections. But no calculated result fits the observed data. Again the LF81 and LF85 interactions give analysing power predictions quite at odds with observation. However, without a reasonable fit to differential cross-section data, any fit to analysing powers must be considered fortuitous.

Clearly, the effective *t*-matrices are quite diverse and consequently DWA predictions of inelastic scattering cross sections, irrespective of how good the microscopic wavefunctions used to give OBDMEs etc., will vary markedly. But

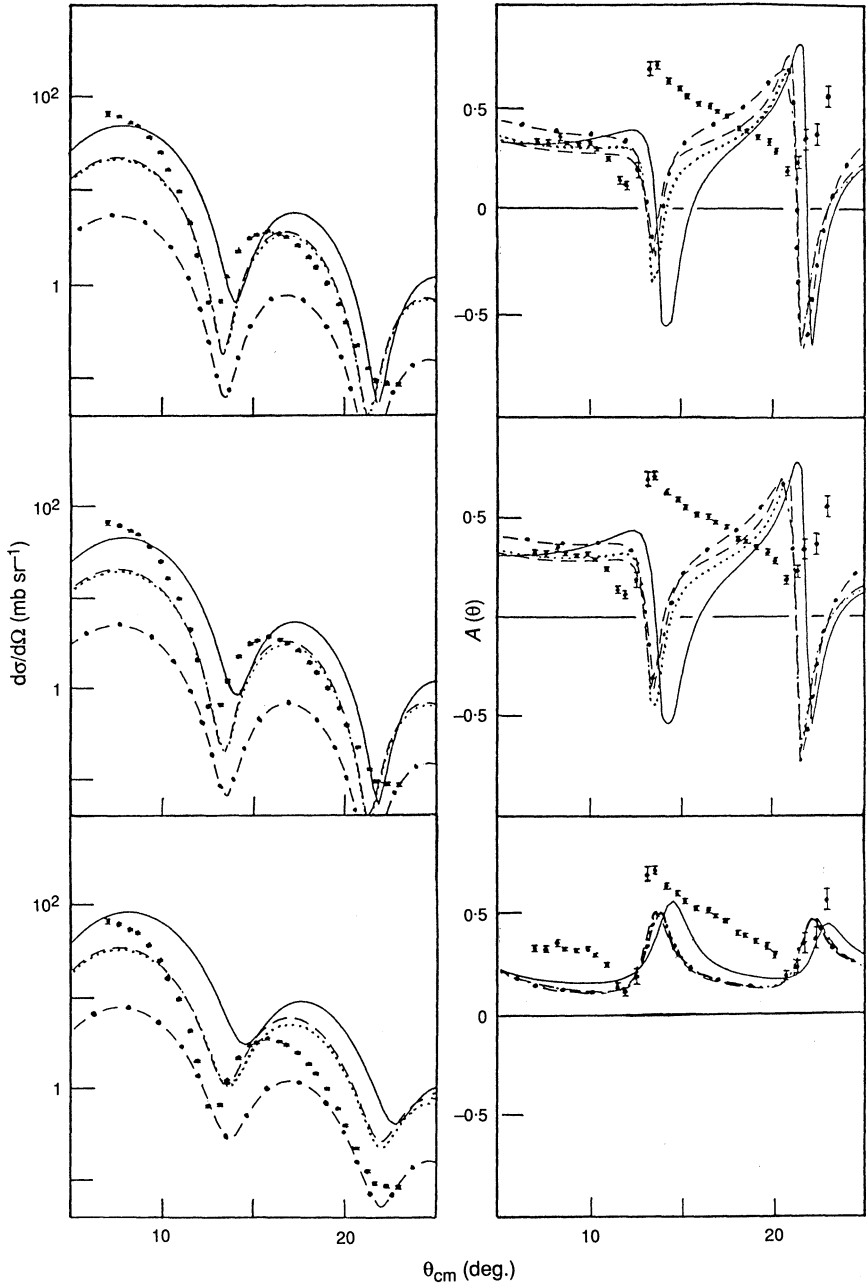


Fig. 2. Data from inelastic scattering of 800 MeV protons from ^{20}Ne leading to the 2_1^+ state, compared with the results from various microscopic model DWA calculations. Details are given in Section 3.

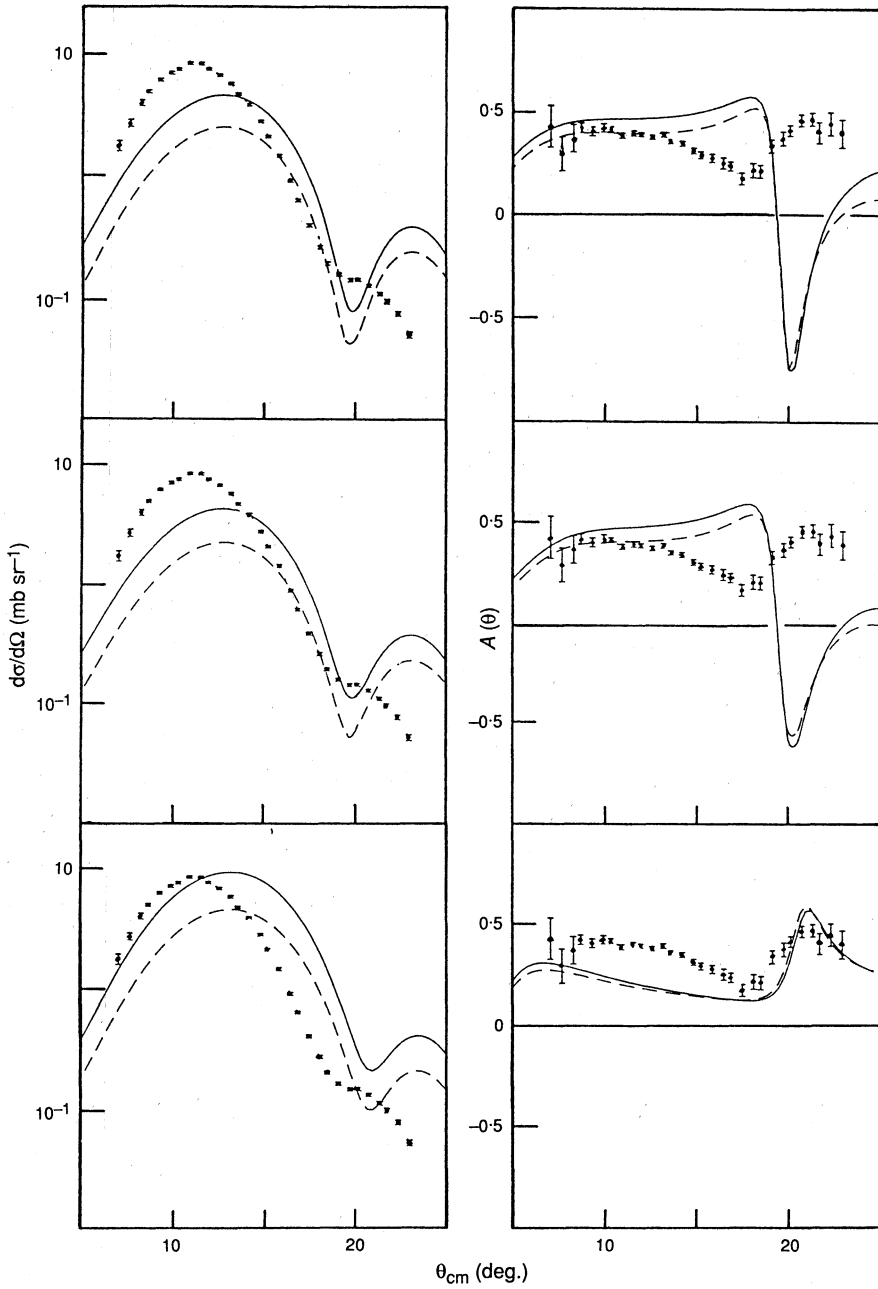


Fig. 3. Comparison of data from excitation of the 4_1^+ state in ^{20}Ne with the results of various microscopic model DWA calculations made using the full basis PHF (continuous curve) and s-d PHF (dashed curve) wavefunctions.

it is a surprise that none of the calculations come close to fitting experiment. A better comparison with data could be obtained by adjusting (lowering) the oscillator energy. Indeed, the electron scattering form factors would fit better with a smaller value of $\hbar\omega$. But to fit the (pp') cross sections a large and quite unrealistic change would be required. We presume, therefore, that we have observed a deficiency with the reaction mechanism. Such a presumption is supported by the magnitudes of the various cross-section data in the momentum transfer regime of 1 to 2 fm⁻¹. The three transitions, elastic, 2_1^+ and 4_1^+ excitations, are all of order 10 mb sr⁻¹. Thus, the premise upon which the DWA is based, namely of dominance in the elastic channel, is not true in this case. Coupled channels must be considered at the very least then, but the existing computer codes are all based upon collective models of structure.

Table 5. Deformation parameters

Reaction	Reference	β_2	$\beta_2 R$	β_4	$\beta_4 R$	β_6	$\beta_6 R$
(e, e')	A	0.4	1.16	0.19	0.55		
(p, p')		0.47	1.35	0.28	0.81		
(α , α')		0.35	1.29	0.11	0.41		
(p, p') 24.5 MeV	B	0.47	1.35	0.28	0.81	-0.1	-0.29
(p, p') 800 MeV	C	0.46	1.32	0.27	0.78	+0.03	+0.09
(p, p') 800 MeV	D	0.65	1.68	0.38	0.98	+0.03	+0.08
(p, p') 800 MeV	E	0.536	1.43	0.318	0.85	-0.12	-0.32

^A Horikawa *et al.* (1971, and references therein). ^B de Swiniarski *et al.* (1976).

^C Blanpied *et al.* (1988). ^D Blanpied *et al.* (1984). ^E Pham and de Swiniarski (1990).

Collective models of structure have been used in analysis of the measured electromagnetic form factors (Horikawa *et al.* 1971). The results of that analysis suggested some hexadecapole deformation in the ground state of ^{20}Ne , with deformation parameters as given in the first row of Table 5. In that study the deformations were compared with parameters obtained using the same model of structure to analyse (low energy) (pp') and ($\alpha\alpha'$) reaction data. For completeness, all those values are listed in Table 5, along with the scale product βR which may be considered more relevant to compare. It is evident that there is some spread in the extracted deformation parameters according to the type of data analysed. But at 800 MeV, previous analyses of inelastic proton scattering data give deformation values much larger than the other low energy data suggest. We repeated the coupled equation calculations for the Ne ground state band using standard form interactions and the results are presented in Fig. 4, with differential cross sections on the left and analysing powers on the right. The results of three different calculations are shown for comparison with the cross-section data, but for only two with the analysing power data. The continuous curves depict DWA collective model results, i.e. no channel coupling. These were obtained by using the standard extended optical model prescriptions for the excitation mechanism and optical potential parameters given by a best fit to the elastic scattering data. The potential parameters and the deformation parameters required to obtain fits to the inelastic scattering are listed in Tables 1 and 5, values previously obtained by Blanpied *et al.* (1984, 1988). The dashed curves are the results obtained using the standard coupled channels approach [program ECIS88 was used (Raynal 1988)], based upon the Schrödinger equation and by allowing coupling between

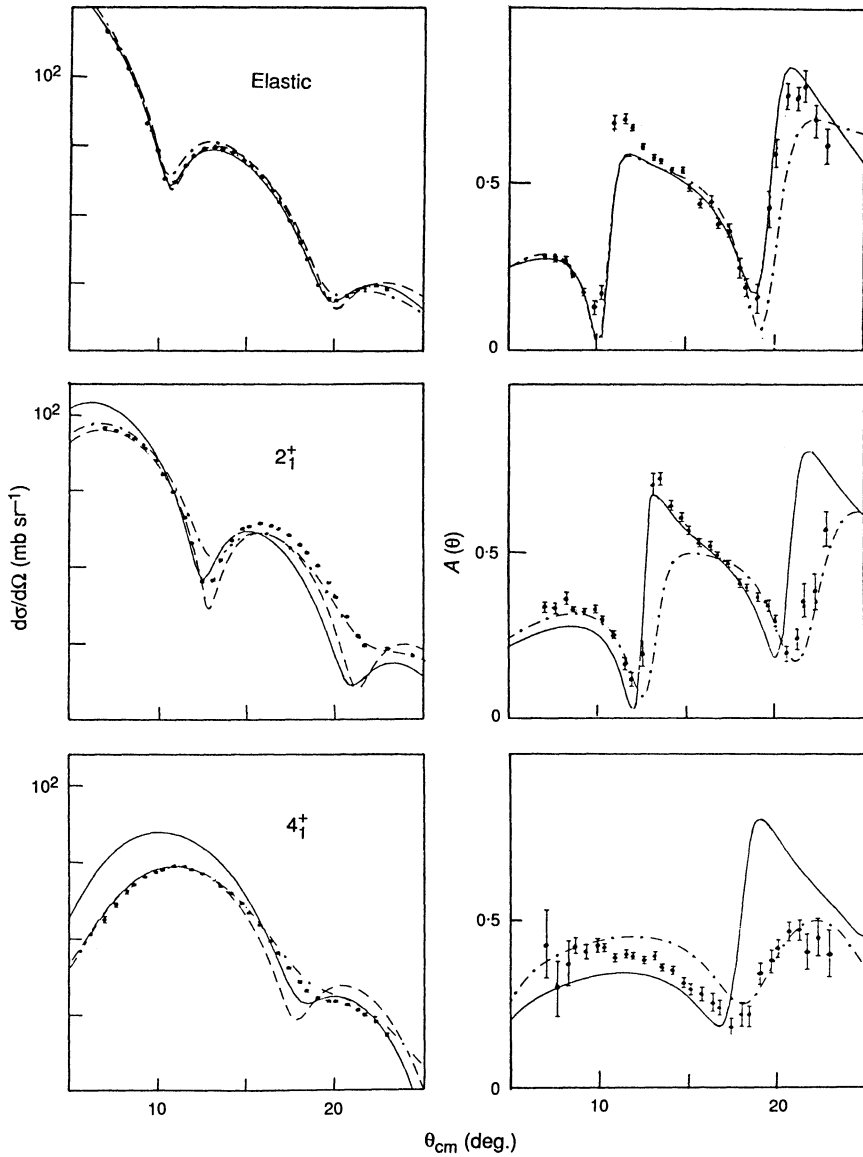


Fig. 4. Differential cross sections and analysing powers from the elastic (top), 2_1^+ (middle) and 4_1^+ (bottom) excitations in ^{20}Ne by 800 MeV protons. The results displayed were obtained using various coupled channels calculations, as described and identified in the text.

the 0_1^+ , 2_1^+ , 4_1^+ and 6_1^+ states. The remaining results displayed in Fig. 4 by the dot-dash curves were obtained using a recent version of ECIS in which the coupled channels calculations are based upon Dirac equations. These results have been considered before (Pham and de Swiniarski 1990), but are repeated here for comparison. The parameter values for both the Schrödinger and Dirac coupled channels calculations are given in Tables 1 and 6 respectively.

Table 6. Dirac optical model potential as defined by de Swiniarski *et al.* (1988)

Term	Real			Imaginary		
	V (MeV)	r (fm)	a (fm)	W (MeV)	r (fm)	a (fm)
Scalar	-199.53	0.98	0.67			
Vector	98.98	1.04	0.61	-80.04	0.90	0.57
Tensor	27.02	0.91	0.70			

In comparison with the microscopic model calculations, these collective model results all give very good fits to the data; albeit the DWA collective model results for the 4_1^+ excitation are noticeably the least satisfactory. Both cross sections and analysing power data are fitted, with the Dirac coupled channels results being preferred to those of Schrödinger coupled channels calculations. But it is the deformation strength that is the most revealing. The DWA collective model results require inordinately large values of β_2 and β_4 (see Table 5). They are far in excess of what the electromagnetic and 24.5 MeV (pp') cross section data require. The coupled channels calculations also require deformation strengths larger than, but not inordinately larger than, the values extracted from low energy data.

4. Conclusions

At 800 MeV, the coupled channels effects are paramount in the reaction mechanism of inelastic proton scattering from ^{20}Ne to the ground state band. In hindsight it seems obvious given that the elastic, 2_1^+ and 4_1^+ cross sections are comparable in magnitude in the region of 1 to 2 fm^{-1} momentum transfer. But the very shape of the distributions, characteristic though they be of the angular momentum transfer in direct scattering, cannot be reproduced by any of the microscopic model calculations. This is in distinct contrast to results obtained with those same microscopic model structure details in analyses of both the electron scattering (longitudinal) form factors and of low energy inelastic proton scattering.

The use of the Dirac rather than the Schrödinger equation coupled channels analyses improves agreement with data as has been noted elsewhere (Pham and de Swiniarski 1990) but, at 800 MeV, the most important facet of the reaction mechanism in this ground state band excitation is channel coupling itself.

Acknowledgments

We are very pleased to present this paper in honour of the sixtieth birthday of Professor I. E. McCarthy. One of us (K. A.) also gratefully acknowledges the many years of fruitful collaboration, and the even longer period of friendship, with Ian.

References

- Amos, K., and Bauhoff, W. (1984). *Nucl. Phys. A* **424**, 60.
- Amos, K., Berge, L., and Kurath, D. (1989*a*). *Phys. Rev. C* **40**, 1491.
- Amos, K., de Swiniarski, R., and Berge, L. (1988). *Nucl. Phys.* **41**, 633.
- Amos, K., Koetsier, D., and Kurath, D. (1989*b*). *Phys. Rev. C* **40**, 374.
- Amos, K. A., and McCarthy, I. E. (1963). *Phys. Rev.* **132**, 2261.
- Amos, K., Nesci, P., and Morrison, I. (1980). *Aust. J. Phys.* **33**, 495.
- Amos, K., and Steward, C. (1990). *Phys. Rev. C* **41**, 335.
- Arndt, R. A., Roper, L. D., Bryan, R. A., Clark, B., Ver West, B. J., and Signell, P. (1983). *Phys. Rev. D* **28**, 97.
- Blanpied, G. S., Balchin, G. A., Langston, G. E., Ritchie, B. G., Barlett, M. L., Hoffmann, G. W., McGill, J. A., Franey, M. A., Gazzaly, M., and Wildenthal, B. H. (1984). *Phys. Rev. C* **30**, 1233.
- Blanpied, G. S., Ritchie, B. G., Barlett, M. L., Ferguson, R. W., Hoffmann, G. W., McGill, J. A., and Wildenthal, B. H. (1988). *Phys. Rev. C* **38**, 2180.
- Cheon, I. T. (1983). *Phys. Lett. B* **124**, 451.
- de Swiniarski, R., Pham, D. L., and Raynal, J. (1988). *Phys. Lett. B* **213**, 247.
- de Swiniarski, R., Sherman, J., Hendrie, D. L., and Bacher, A. D. (1976). *Helv. Phys. Acta* **49**, 241.
- Ford, W. C., Braley, R. C., and Bar-touv, J. (1971). *Phys. Rev. C* **4**, 2099.
- Horikawa, Y., Torizuka, Y., Nakada, A., Kojima, Y., and Kimura, M. (1971). *Phys. Lett. B* **36**, 9.
- Lacombe, M., Loiseau, B., Richard, J. M., Vinh-Mau, R., Côte, J., Pirès, P., and de Tournell, R. (1980). *Phys. Rev. C* **21**, 861.
- Love, W. G., and Franey, M. A. (1981). *Phys. Rev. C* **24**, 1073.
- Love, W. G., and Franey, M. A. (1985). *Phys. Rev. C* **31**, 483.
- Millener, D. J., Sober, D. I., Crannell, H., O'Brien, J. T., Fagg, L. W., Kowalski, S., Williamson, C. F., and Lapikas, L. (1989). *Phys. Rev. C* **39**, 14.
- Nesci, P., and Amos, K. (1977). *Nucl. Phys. A* **284**, 239.
- Pham, D. L., and de Swiniarski, R. (1990). *Z. Phys. A* **335**, 37.
- Raynal, J. (1987). *Phys. Lett. B* **196**, 7.
- Raynal, J. (1988). Proc. Workshop on Applied Nuclear Theory and Nuclear Model Calculations for Nuclear Technology Applications (ICTP: Trieste).
- von Geramb, H. V., (1983). 'The Interaction between Medium Energy Nucleons and Nuclei', AIP Conf. Proc. No. 97 (Ed. H. O. Meyer), p. 44 (AIP: New York).
- von Geramb, H. V., and Amos, K. A. (1990). *Phys. Rev. C* **41**, 1384.